Subreflector Focusing Techniques Applied to New DSS-15 and DSS-45 34-Meter Antennas

R. D. Hughes and M. S. Katow
Ground Antennas and Facilities Engineering Section

An improved technique for determining the subreflector translations required to properly focus a Cassegrainian antenna, under gravity loading, at a full range of elevation angles, is presented. This technique is applied to the 34-m antenna configuration installed at stations DSS-15 (Goldstone, California) and DSS-45 (Australia). The subreflector lateral and axial translations, to be stored into the antenna-control systems, are computed and tabulated. The relationships that govern the main parameters are also presented for future subreflector focusing analysis under wind and thermal loadings.

I. Introduction

Future upgrades and the improved gain/noise ratio (G/T) operation of the Deep Space Network (DSN) antennas at X-band and at higher frequencies has created stringent requirements for maintaining minimum dimensional tolerances of various major components for precision motion. The subreflector position controller (s) is a key component in improving focusing. A refined technique has been developed to accurately determine the subreflector focusing motions as a function of the antenna elevation angle. The resulting subreflector motions are effected by the microprocessor-controlled subreflector servo-positioner mechanism in order to maximize antenna gain by compensating for gravity-induced deformations as the elevation angle changes.

As with techniques conventionally used in the past, the new technique involves ray tracing using geometric optics to compute the required subreflector motions through the full range of elevation angles. However, new procedures have been included such that the antenna's secondary virtual focus coincides, after focusing is completed, with the main reflector's "best-fit" focus, as shown in Fig. 1. The system's "best-fit" parameters are determined according to the best-fit reflector configuration (still a paraboloid). The latter is the best approximation, by the least-squares method, of the deformed main reflector at a given elevation angle (Ref. 1). Figure 1 also shows the reference coordinate-system orientation used in our analysis. Tables 1 and 2 show lateral (Y) and axial (Z) subreflector offsets as a function of the antenna elevation angle. (The results of the IDEAS structure program analysis will be entered into the subreflector control logic.) These offset tables will provide initial positioning data which may be refined in the future as the antennas are calibrated using the known star-tracking procedure.

Although the 34-m antennas have "shaped" main and subreflectors, the use of a close-fitting paraboloid for the analysis in this study should provide accurate answers.

II. Analysis

The 34-m AZ-EL antenna design for both stations is structurally identical. The parameters describing the deformed antenna configuration under varying gravity loadings were studied both analytically and experimentally. First, structural deflections were modeled by the finite-element method using JPL's IDEAS computer program (Ref. 2). Relative motions of major antenna components with respect to the computed best-fit paraboloid were determined (Ref. 1). Second, subreflector motions relative to the quadripod apex, which were due to the subreflector positioner mechanism deflections, were determined by measurements. A test fixture was constructed, by the vendor (TIW at Sunnyvale, California), to carry the subreflector and the positioner mechanism. This fixture was tipped at various angles, simulating elevation angle changes of the antenna and/or the subreflector. Use of this test fixture data is discussed later on for individual loading cases.

The results of the IDEAS computer program were obtained for two cases: (1) Y-gravity loading with a unit gravity load (1.0**g**, where **g** is the acceleration of gravity) is applied in the Y-direction to simulate antisymmetric loading conditions when the antenna is oriented in the horizon position ($E = 0$, where E is the elevation angle); and (2) Z-gravity loading with unit gravity load (1.0**g**) applied in the Z-direction to simulate the symmetric loading conditions when the antenna is in the zenith-look position ($E = 90^\circ$).

The major components of the Cassegrainian antenna, with the exception of the subreflector positioner mechanism, act together as a single elastic structure under gravity loading. Therefore, the principle of superposition may be applied, and the following relationships exist for subreflector positioning:

$$\text{Axial correction} = \Delta Z = \Delta Z_0 \,(\sin E - \sin E_r) \qquad (1)$$

$$\text{Lateral correction} = \Delta Y = \Delta Y_0 \,(\cos E - \cos E_r) \qquad (2)$$

where

ΔZ_0 = axial correction required for unit (1.0**g**) Z-direction load

ΔY_0 = lateral correction required for unit (1.0**g**) Y-direction load

E = antenna elevation angle

E_r = antenna-rigging angle, the elevation angle at which the main reflector panels are set in the field to ideally form an undistorted paraboloid surface

The beam deviation or reflection ratio, K, is defined as the "cumulative" ratio of the angle of reflection to the angle of incidence of the "transmitted" beam rays. This ratio, K, is not equal to unity due to the nature of the RF radiation pattern in this type of antenna. The beam deviation or reflection ratio, K, is determined from Fig. 2, taken from Ref. 3. Figure 2 relates various antenna performance parameters to the ratio of the main reflector focal length to the aperture diameter (F/D), and was constructed using the JPL Radiation Program as described in detail in Ref. 3. For the 34-m antenna, under study, $F/D = 0.324$, which gives $K = 0.775$. The following two extreme gravity-loading cases are presented in order to determine the subreflector focusing parameters at any elevation angle between 0° and 90°.

A. Gravity Loading at Zenith Look

Figure 3 illustrates the geometry of the deflections involved in the Z-gravity loading case. The known parameters in Fig. 3, obtained from the design configuration and the computer model are:

f = design focal length = 1102.36 cm (434.0 in.)

f' = "best-fit" focal length = 1101.93 cm (433.83 in.)

U = "best-fit" main-reflector vertex axial offset = 0.373 cm (0.147 in.)

V = subreflector vertex axial offset = 0.417 cm (0.164 in.)

W = axial displacement of the main reflector focus = $(f - f' - U)$ = 0.058 cm (0.023 in.)

Z = required axial subreflector translation for unit (1.0**g**) gravity load in $+Z$-direction = $e + d$ = 0.475 cm (0.187 in.)

To illustrate the concept of having an effective gravity load in the $+Z$-direction, suppose that the antenna was "rigged" at zenith, then moved to horizon. The net change in gravity loading would be 1.0**g** in the $+Z$-direction, and the subreflector would have to be moved axially, toward the main reflector, for proper focusing since the main reflector becomes deeper. Equation (1) follows this behavior.

Table 1 lists the required total axial-focusing translations as a function of the elevation angle, for a rigging angle of 45°. The tabulated values were obtained by adding the measured positioner-mechanism axial deflections to the ΔZ values obtained by using Eq. (1) at each elevation angle (with ΔZ_0 = 0.475 cm). Since the positioner-mechanism deflections were originally measured relative to horizon-loading conditions, the measured values indicated in Table 1 have been redefined in terms of a 45° rigging angle. Linear interpolation was used to determine the positioner-deflection corrections at intermediate angles. Note that the net ΔZ from the horizon to zenith positions (0.686 cm or 0.270 in.) indicated in Table 1 is equal to the sum of ΔZ_0 and the net positioner deflection, i.e., (0.475 + 0.0457 + 0.1651) cm.

B. Gravity Loading at Horizon Look

Figure 4 illustrates the geometry of the antenna deflections in the Y-gravity loading case. The known design parameters are:

a = length from subreflector vertex to primary design focus = 541.54 cm (213.206 in.)

b = length from subreflector vertex to secondary design focus = 69.35 cm (27.305 in.)

f = design reflector focal length = 1102.36 cm (434.0 in.)

d = feed lateral displacement = 0.983 cm (0.387 in.)

e = main reflector vertex lateral displacement = 3.439 cm (1.354 in.)

β = angular displacement of "best-fit" focal axis = 0.002577 rad

From the combined computer model deflections and measured deflections of the subreflector positioner one obtains

c = subreflector vertex lateral translation = 3.084 cm (1.214 in.)

α = subreflector focal axis angular displacement = 0.00169 rad

Focal length changes for this case are relatively small and are considered negligible. From the geometry shown in Fig. 4, the remaining parameters may be calculated as follows:

$m = \alpha a$ = 0.914 cm (0.360 in.)

$n = c + m - d$ = 3.015 cm (1.187 in.)

$\delta = n/a$ = 0.00557 rad

$W = \delta b$ = 0.386 cm (0.152 in.)

$P = b\alpha$ = 0.1171 cm (0.0461 in.)

$q = c - p - w$ = 2.581 cm (1.016 in.)

$r = \beta f$ = 2.840 cm (1.118 in.)

$s = e - r$ = 0.599 cm (0.236 in.)

$t = q + s$ = 3.180 cm (1.252 in.)

$h = tk$ = 2.464 cm (0.970 in.)

$\gamma = (r - h)/f = 0.000341°$ (1.17 arc sec)

The angle, γ, is the boresight-pointing error due to subreflector lateral misalignments. The computational procedure performed above may be applied in general to AZ-EL antennas to determine the boresight-pointing error due to lateral subreflector misalignments.

The focused antenna configuration for the y-gravity loading case is shown in Fig. 5, where Δy_0 is the required subreflector translation. The known quantities in the figure are: a, b, d, s, and α. There are three unknown quantities: θ, ℓ, and g. By simple geometric analysis, the following equations may be derived:

$$\theta = (g - d)/a \tag{3}$$

$$\ell = \alpha (a + b) - g \tag{4}$$

$$\theta = (s - \ell)/b \tag{5}$$

Since ℓ is the only unknown pertaining directly to Δy_0, Eqs. (3), (4), and (5) were combined so that θ and g were eliminated, and the following expression for ℓ is obtained:

$$\ell = \frac{1}{1 - a/b}\left[\alpha(a + b) - \frac{a}{b} S - d\right] \tag{6}$$

For this case, ℓ = 0.681 cm (0.268 in.). The required subreflector translation is:

$$\Delta y_0 = \ell + c - p \tag{7}$$

By referring to Figs. 4 and 5, then

$$\Delta y_0 = 3.647 \text{ cm (1.436 in.)}$$

It should be noted that in this case, the subreflector vertex lateral deflection (c = 3.084 cm) was calculated by taking into account the measured deflection and rotation of the subreflector due to positioner-mechanism flexibilities, as well as the computer model results for apex translation and rotation. The required subreflector lateral translations, as a function of the elevation angle, were obtained using Eq. (2), and are presented in Table 2. The measured positioner-mechanism lateral deflections were taken into account by incorporation of the zenith-to-horizon deflection in Δy_0, instead of by reperforming the entire computational procedure at each elevation angle. This modified approach avoids unnecessary computations and provides accurate results, since the positioner-mechanism lateral deflection trend changes similar to $\cos\theta$ as the elevation angle changes.

III. Summary

For two 34-m diameter AZ-EL-type Cassegrainian antennas, a refined analysis was made to determine the boresight-pointing error, lateral, and axial translations required to properly focus the subreflector as a function of the antenna elevation angle. Deformations of the components comprising the antenna must be quantified for zenith and horizon gravity-loading conditions. This analysis was applied to the 34-m antenna configuration most recently installed at the two tracking stations DSS-15 and DSS-45.

By utilizing Eqs. (1) and (2) with the appropriate geometric relationships the required subreflector translations for other types of loads, e.g., wind or thermal, may be determined in a similar fashion using this new procedure.

References

1. Katow, M. S., and Schmele, L. W., "Antenna structures: Evaluation Techniques of Reflector Distortions," *Space Programs Summary*, Special Publication Summary 37-40, Vol. IV, pp. 176–184, Jet Propulsion Laboratory, Pasadena, CA, September, 1968.
2. Levy, R., "Optimization of Antenna Structure Design," *Eighth Conference on Electronic Computation*, ASCE, pp. 114–129, Houston, Texas, Feb., 1983.
3. Katow, M. S., "34-Meter Antenna – Subreflector Translations to Maximize RF Gain," *TDA Progress Report 42-62*, pp. 112–120, Jet Propulsion Laboratory, Pasadena, CA, January and February, 1981.

Table 1. Required axial (Z) subreflector correction as a function of the elevation angle (rigging angle = 45°)

Elevation angle (deg)	Positioner correction (measured) cm (in.)		Total correction cm (in.)	
90 (zenith)	0.0457	(0.018)	0.185	(0.073)
85	0.0203	(0.017)	0.180	(0.071)
80	0.0406	(0.016)	0.173	(0.068)
75	0.0381	(0.015)	0.161	(0.063)
70	0.0330	(0.013)	0.144	(0.057)
65	0.0254	(0.010)	0.120	(0.047)
60	0.0203	(0.008)	0.096	(0.038)
55	0.0127	(0.005)	0.066	(0.026)
50	0.0076	(0.003)	0.035	(0.014)
45	0	(0)	0	(0)
40	-0.0178	(-0.007)	-0.048	(-0.019)
35	-0.0356	(-0.014)	-0.099	(-0.039)
30	-0.0533	(-0.021)	-0.152	(-0.060)
25	-0.0711	(-0.028)	-0.206	(-0.081)
20	-0.0914	(-0.036)	-0.264	(-0.104)
15	-0.1118	(-0.044)	-0.325	(-0.128)
10	-0.1270	(-0.050)	-0.381	(-0.150)
5	-0.1473	(-0.058)	-0.442	(-0.174)
0 (horizon)	-0.1651	(-0.065)	-0.501	(-0.197)
Net, horizon-to-zenith motion	0.2108	0.083	0.686	0.270

Table 2. Required lateral (Y) subreflector corrections as a function of the elevation angle (rigging angle = 45°)

Elevation angle (deg)	Correction cm (in.)	
90 (zenith)	-2.578	(-1.015)
85	-2.261	(-0.890)
80	-1.943	(-0.765)
75	-1.633	(-0.643)
70	-1.331	(-0.524)
65	-1.036	(-0.408)
60	-0.754	(-0.297)
55	-0.488	(-0.192)
50	-0.234	(-0.092)
45	0	0
40	0.211	(0.083)
35	0.409	(0.161)
30	0.579	(0.228)
25	0.726	(0.286)
20	0.851	(0.335)
15	0.945	(0.372)
10	1.013	(0.399)
5	1.054	(0.415)
0 (horizon)	1.069	(0.421)

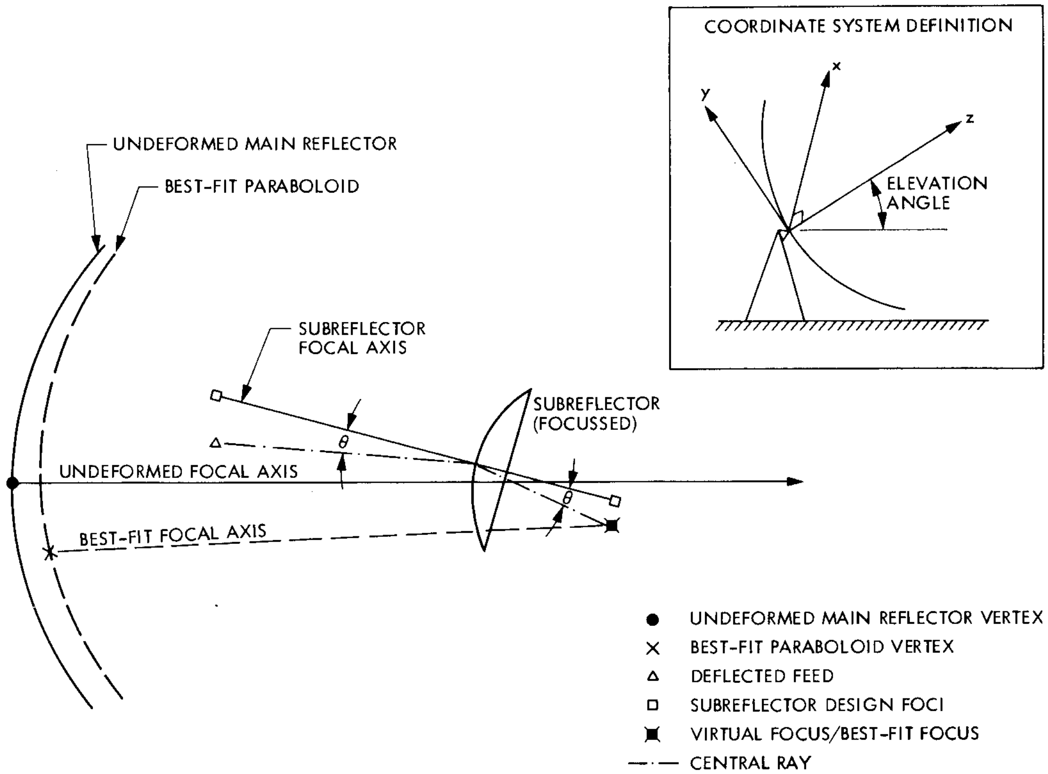

Fig. 1. Focused Cassegrainian geometry, with best-fit parabola

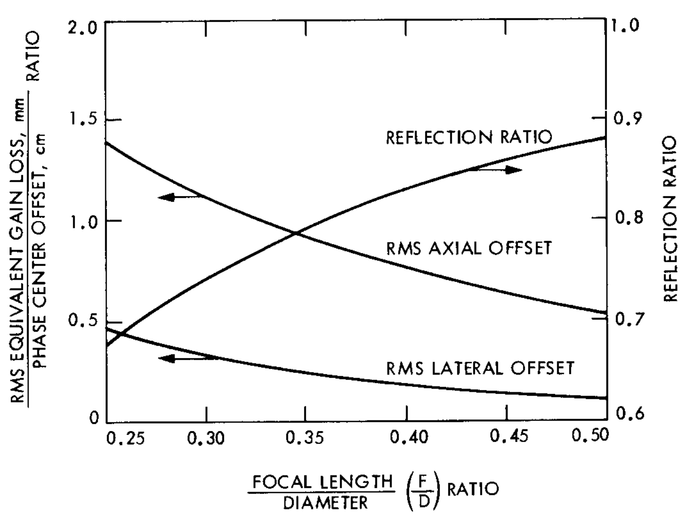

Fig. 2. Antenna gain reduction and reflection ratio as a function of the subreflector offset and paraboloid F/D ratio

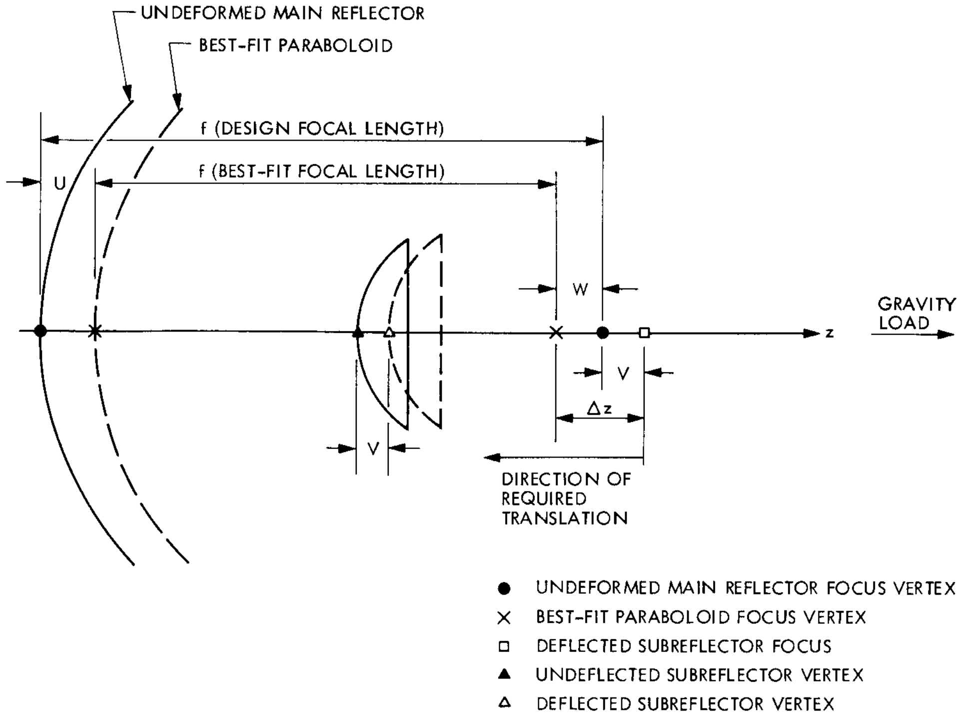

Fig. 3. Deflections and translations for zenith loading

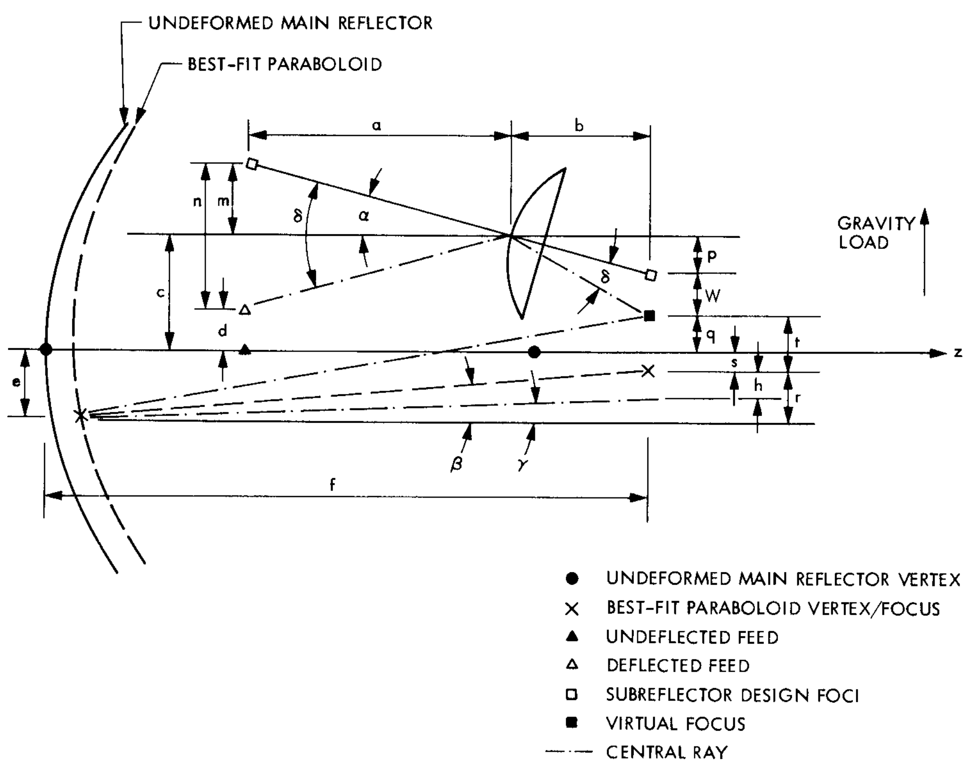

Fig. 4. Deflections for horizon loading

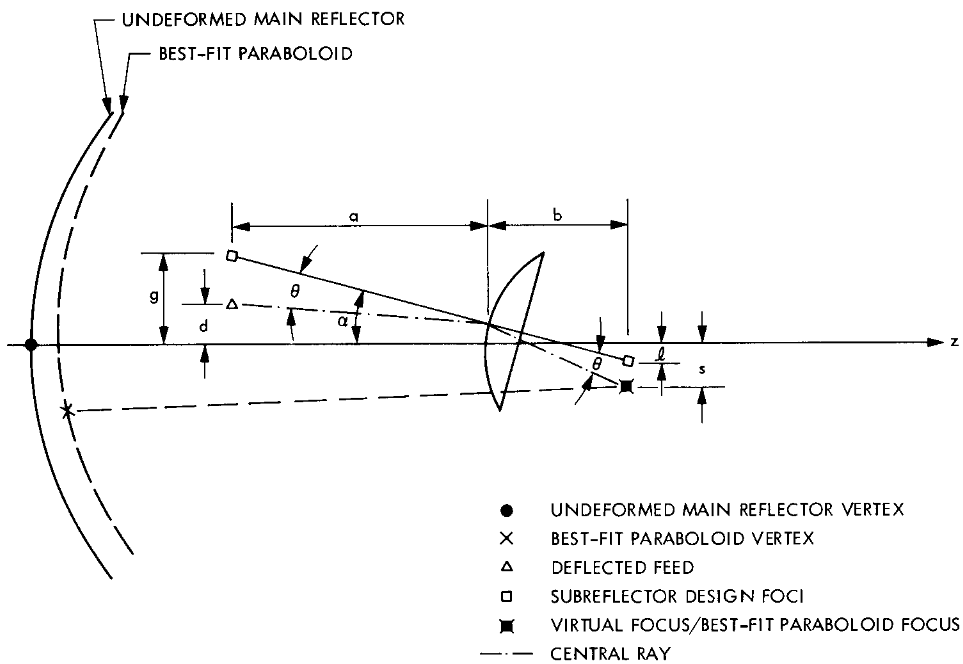

Fig. 5. Focused configuration for horizon loading